LQG Control of Hybrid Foil-Magnetic Bearing

Tian Ye[1,a], Sun Yanhua[1,b] , Yu Lie[1,c]
[1]Institute of Mechatronics and Information Systems,
Key Laboratory of Ministry of Education for Strength and Vibration
Xi'an Jiaotong University, Xi'an, 710049, China
[a]tony_kk@stu.xjtu.edu.cn, [b]sunyanhua@mail.xjtu.edu.cn, [c]yulie@mail.xjtu.edn.cn

Abstract: A hybrid foil magnetic bearing is a combination of the foil bearing and magnetic bearing, which have the advantages of both and can also share loads between them. In this paper, the model of a rigid rotor supported by two hybrid foil magnetic bearings was established, and a controller based on the Linear Quadratic Gaussian control law was designed for this new type of bearing. Finally, Simulation was performed to verify the performance of the rotor-bearing system, and the results show that the system could work well at situations with strong perturbation forces.

Introduction

Active magnetic bearings (AMBs) are most commonly used magnetic bearings which generate magnetic forces to support rotor. AMBs need no lubrication and sealing, and wear is completely eliminated. The dynamics of a rotor supported by AMBs can be actively controlled by adjusting the stiffness and damping of the bearing. However, because of flux saturation in the iron, thermal effect, and etc., load capacity of the magnetic bearing can not be increased further. Moreover, as the rotation speed is very high, the whole system might be apt to destabilized due to time delay of the digital controller[1]. Foil bearings(FBs) provide another contact-free way to support high speed rotor. They have favorable self-adaptability, and can work for long time even under high temperature, high-speed and high-polluted conditions. The foil bearing has very simple structure and also need no lubrication, The disadvantage of the foil bearing is relatively lower load capacity compared to other bearings Moreover, at the stage of system startup and shutdown, friction and wear between the journal and the top foil are inevitable, which will reduce the life of foil bearings greatly [2-5]. A hybrid foil magnetic bearing(HFMB) is a combination of the foil bearing and magnetic bearing, which have the advantages of both bearings, and can share loads between them also. It can not only improve the load capacity but also the dynamic damping and stiffness of the rotor-bearing system. Therefore, the HFMB is ideal to support high-speed rotors.

In this paper, a model of the HMFB with four DOFs was established, and the Linear-Quadratic-Gaussian control (LQG) was designed based on this model. The LQG control could make the hybrid magnetic-foil bearing work well under system noise and sensor noise.

1. Hybrid foil-magnetic bearing

The structure of the HFMB mentioned in this paper is shown in Fig. 1. The foil bearing consists of four top foils each supported by a bottom bump foil and located in the airgap between the stator and rotor of the magnetic bearing. Therefore, the airgap of the AMB is larger (about 0.8mm) in order to contain the foil bearing, and the foils are made of non magnetic materials so that it will not affect the work of the AMB. It is assumed that the two bearings are working independently.

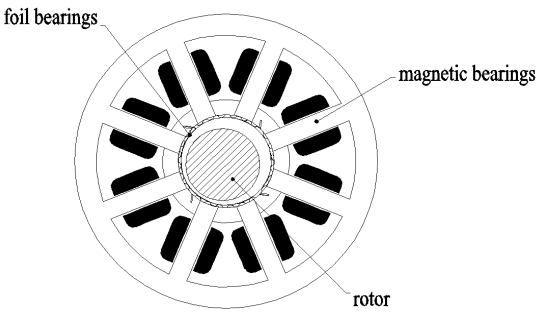

Fig.1 Structure of the HFMB

For the magnetic bearing, it is usually differentially configured in each of the two controlled directions x and y. The magnetic bearing can be modeled by the force-displacement stiffness k_{xx}、k_{yy} and force-current stiffness k_{xi}、k_{yi}, and they can be easily calculated with the design parameters of the magnetic bearing[6]. The dynamic characteristics of the foil bearing can be represented by four stiffness and four damping coefficients which can be obtained by solving Reynolds equation [7] . These coefficients can be written as $k_{fxx}, k_{fxy}, k_{fyx}, k_{fyy}, d_{xx}, d_{xy}, d_{yx}, d_{yy}$.

2. Rotor-bearing system model

When the ratio of the rotor length to the diameter of the thrust disc is relatively large, influences of the thrust bearing to radial motion of the rotor can be neglected [6]. Therefore, the axial motion of the rotor could be studied separately. A rigid rotor supported only by two radial bearings as shown in Fig.2 is discussed in this paper.

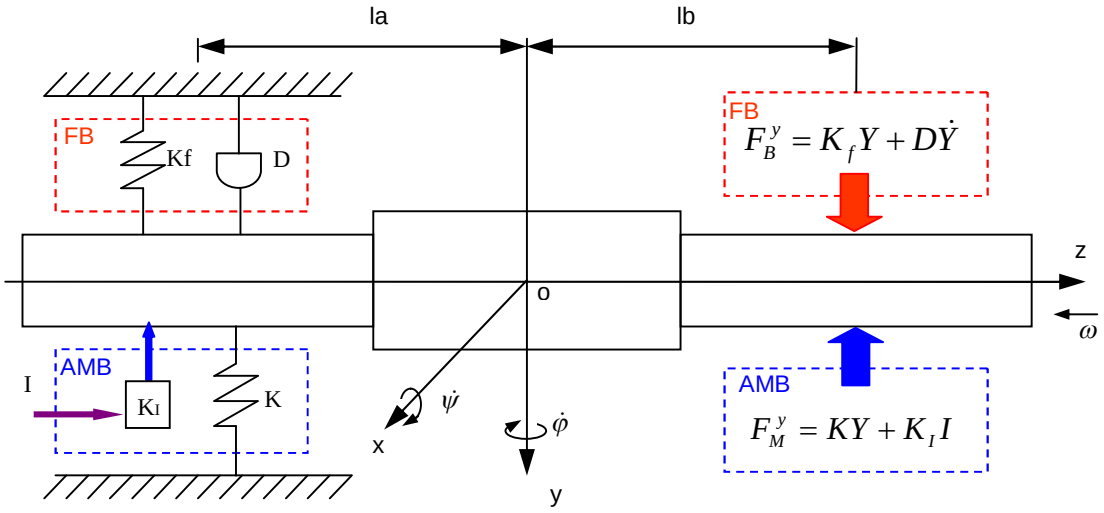

Fig. 2 Rigid rotor model

l is the distance between the two radial bearings and o is the mass center of the rotor. The generalized displacements are defined as $q = [x, y, \varphi, \psi]^T$, where x and y are the displacements of its center of mass o with respect to the inertial reference and φ and ψ are the angular motion around the y and x axis. The radial displacements of the journal at bearing positions are defined as: $q_B = [x_a, x_b, y_a, y_b]^T$. The equations of motion of the rotor are:

$$\begin{cases} m\ddot{x}_g + \Delta F_{xa} + \Delta F_{xb} = f_x \\ m\ddot{y}_g + \Delta F_{ya} + \Delta F_{yb} = f_y \\ J_y\ddot{\varphi}_g + \omega J_z\dot{\psi}_g = l_a\Delta F_{xa} - (l-l_a)\Delta F_{xb} \\ J_x\ddot{\varphi}_g - \omega J_z\dot{\psi}_g = l_a\Delta F_{ya} - (l-l_a)\Delta F_{yb} \end{cases} \quad \begin{cases} \Delta F_{xa} = k_{xx}^a x_a + k_{fxx}^a x_a + k_{fyx}^a y_a + d_{xx}^a \dot{x}_a + d_{yx}^a \dot{y}_a + k_{xi}^a i_{xa} \\ \Delta F_{xb} = k_{xx}^b x_b + k_{fxx}^b x_b + k_{fyx}^b y_b + d_{xx}^b \dot{x}_b + d_{yx}^b \dot{y}_b + k_{xi}^b i_{xb} \\ \Delta F_{ya} = k_{yy}^a y_a + k_{fyy}^a y_a + k_{fxy}^a x_a + d_{yy}^a \dot{y}_a + d_{xy}^a \dot{x}_a + k_{yi}^a i_{ya} \\ \Delta F_{yb} = k_{yy}^b y_b + k_{fyy}^b y_b + k_{fxy}^b x_b + d_{yy}^b \dot{y}_b + d_{xy}^b \dot{x}_b + k_{yi}^b i_{yb} \end{cases} \quad (1)$$

where, m is the mass of the rotor, ω is the rotational speed, $\Delta F_{xa}, \Delta F_{xb}, \Delta F_{ya}$ and ΔF_{yb} are bearing forces in the *x* and *y* directions, f_x and f_y are the external forces, i_{xa}, i_{xb}, i_{ya} and i_{yb} are the control currents, $k_{xx}^a, k_{xx}^b, k_{yy}^a$ and k_{yy}^b are the force-displacement stiffness and $k_{xi}^a, k_{xi}^b, k_{yi}^a$ and k_{yi}^b are force-current stiffness of the magnetic bearings, $k_{fxx}^a, k_{fxy}^a, k_{fyx}^a, k_{fyy}^a, k_{fxx}^b, k_{fxy}^b, k_{fyx}^b$ and k_{fyy}^b are the eight stiffness coefficients of the foil bearings and $d_{xx}^a, d_{xy}^a, d_{yx}^a, d_{yy}^a, d_{xx}^b, d_{xy}^b, d_{yx}^b$ and d_{yy}^b are the eight damping coefficients. The equations of motion can be written as:

$$M\ddot{q} + G\dot{q} + Kq + K_I I = F \quad (2)$$

When the external forces are not considered, Eq. 2 can be expressed as:

$$\ddot{q} = -M^{-1}G\dot{q} - M^{-1}Kq - M^{-1}K_I I \quad (3)$$

Let $X = \begin{Bmatrix} q_B \\ q_B' \end{Bmatrix}$, $U = I_B$ and $Y = q_B$, then the state space description of the rotor-bearing system would be:

$$\begin{cases} \dot{X} = AX + BU \\ Y = CX + DU \end{cases}, \quad A = \begin{bmatrix} 0_{4\times4} & I_{4\times4} \\ -M_B^{-1}K_B & -M_B^{-1}G_B \end{bmatrix} B = \begin{bmatrix} 0_{4\times4} \\ -M_B^{-1}K_{IB} \end{bmatrix} C = [I_{4\times4},\ 0_{4\times4}]\ D = 0 \quad (4)$$

3. LQG controller

LQG controller belongs to centralized-control, and it has many advantages compared to decentralized PID control always used in AMB. The feedback matrix *K* given by linear quadratic (LQ) law has simple structure [8]. Furthermore, since not all the state variables can be detected, a state observer is needed to reconstruct the undetected state variables. Fortunately, the *Kalman* filter in LQG controller can be used as a state observer and can suppress the white noise. So, LQG controller is a good choice for the HFMB. The structure of the LQG controller is shown in Fig. 3 [9].

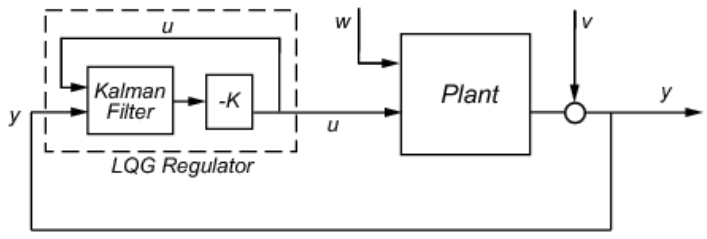

Fig. 3 Structure of the LQG controller

The performance functional of the LQ control is

$$J = \int_0^\infty \left[X^T QX + U^T RU \right] dt \tag{5}$$

where X is the error vector, U is the input vector Q is a positive semi-definite state weighted matrix and R is a positive definite control weighted matrix. Q and R are usually diagonal matrices with element q_i and r_i. If U is the control voltage or current, the second term of the integrand in Eq.5 represents energy consumed during the control process.

Assume that control $U^*(t)$ makes J reach the minimum, and $U^*(t)$ can be expressed as:

$$U^*(t) = -KX_1(t) \tag{6}$$

where $K = R^{-1}B^T P$ is the optimal feedback gain matrix. P is the solution of the following *Riccati* equation:

$$-PA - A^T P + PBR^{-1}B^T P - Q = 0 \tag{7}$$

Therefore, choosing different matrixes Q and R can obtain different optimal feedback matrix K.

Since the LQ control needs full state feedback, a *Kalman* filter can be used to rebuild the state variables if the rotor-bearing system is completely observable. The state equation including system noise and sensor noise is [10]:

$$\begin{aligned} \dot{x} &= Ax + Bu + Gw \\ y_v &= Cx + Du + Hw + v \end{aligned} \tag{8}$$

where w is system noise and v is sensor noise, and both w and v are white noises and satisfy:

$$\begin{aligned} E(w) = E(v) = 0; E(ww^T) = Q_n \\ E(vv^T) = R_n; E(wv^T) = N_n \end{aligned} \tag{9}$$

The *Kalman* filter ξ can be designed as follows

$$\begin{aligned} \dot{\hat{x}} &= A\hat{x} + Bu + L(y_v - C\hat{x} - Du) \\ \begin{bmatrix} \hat{y} \\ \hat{x} \end{bmatrix} &= \begin{bmatrix} C \\ I \end{bmatrix} \hat{x} + \begin{bmatrix} D \\ 0 \end{bmatrix} u \end{aligned} \tag{10}$$

where

$$L = \left(PC^T + \bar{N} \right) \bar{R}^{-1} \tag{11}$$

is the observer gain, and

$$\bar{R} = R_n + HN_n + N_n^T H^T + HQ_n H^T; \bar{N} = G\left(Q_n H^T + N_n \right) \tag{12}$$

Finally, the LQG regulator with the *Kalman* filter and the optimal feedback matrix K in series forms the closed loop feedback control of the rotor-bearing system.

4 Simulation

A HFMB test rig for a *100kW* permanent magnet synchronous motor was designed and its performance is simulated in this paper. The first bending frequency of the rotor is about 1270*Hz*, which is almost 1.8 times of the rated rotation speed 700*Hz*. Therefore, the rotor can be considered as rigid rotor. The parameters of the rotor and HFMB are in table 1. It is assumed that the equilibrium position of the magnetic bearing has already adjusted to the working point of the foil bearing at each rotational speed. The eight stiffness coefficients and eight damping coefficients of the foil bearing are in table 2 [11].

Table 1 parameters of the rotor and HFMB

Rotor mass	m=12.4kg
Distance between mass center and bearing A	la=-210mm
Distance between mass center and bearing B	lb=210mm
Air gap of the magnetic bearing	C_0=0.8mm
Bias current of the magnetic bearing	I_0=4A
Cross-sectional area of the air gap	$Aa = 4.534\times10^{-4} m^2$
Number of turns per coil	N=97
Moment of inertia about the rotational axis	$Jz = 6.88\times10^{-3} kg\cdot m^2$
Moments of inertia in lateral	$Jx = Jy = 2.22\times10^{-1} kg\times m^2$
Rotation speed	ω=42000rpm

Table 2 Dynamic characteristics of the HFMB

Stiffness of the foil bearing (x10^{6}N/m)	Damping of the foil bearings (x10^{2}N·s/m)	Displacement stiffness of the magnetic bearings (x10^{5}N/m)
k^a_{fxx}=3.890	d^a_{xx}=3.9688	$k^a_{xx}=k^a_{yy}$ $=k^b_{xx}=k^b_{yy}$ =-4.651
k^a_{fxy}=1.336	d^a_{xy}=0.8222	
k^a_{fyx}=0.963	d^a_{yx}=-1.204	
k^a_{fyy}=5.447	d^a_{yy}=3.2928	Current stiffness of the magnetic bearings (N/A)
k^b_{fxx}=5.714	d^b_{xx}=4.003	
k^b_{fxy}=1.811	d^b_{xy}=0.8104	$k^a_{xi}=k^a_{yi}$ $=k^b_{xi}=k^b_{yi}$ =102.325
k^b_{fyx}=1.365	d^b_{yx}=-1.177	
k^b_{fyy}=7.548	d^b_{yy}=5.700	

Take these parameters into Eq. 4, the state space matrices *A*,*B*,*C* and *D* of the rotor-bearings system can be derived as:

$$A=\begin{bmatrix} 0 & 0 & 0 & 0 & 1 & 0 & 0 & 0 \\ 0 & 0 & 0 & 0 & 0 & 1 & 0 & 0 \\ 0 & 0 & 0 & 0 & 0 & 0 & 1 & 0 \\ 0 & 0 & 0 & 0 & 0 & 0 & 0 & 1 \\ -981825 & 633297 & -276752 & 165219 & -111.99 & 46.43 & -34.48 & 54.22 \\ 414827 & -1498904 & 116929 & -391044 & 47.31 & -109.9 & 53.92 & -35.18 \\ -383280 & 219236 & -1457111 & 874267 & 45.30 & -58.54 & -92.71 & 67.41 \\ 161938 & -518894 & 615639 & -2069239 & -58.50 & 45.40 & 39.17 & -159.55 \end{bmatrix},\quad B=\begin{bmatrix} 0 & 0 & 0 & 0 \\ 0 & 0 & 0 & 0 \\ 0 & 0 & 0 & 0 \\ 0 & 0 & 0 & 0 \\ 28.57 & -12.07 & 0 & 0 \\ -12.07 & 28.57 & 0 & 0 \\ 0 & 0 & 28.57 & -12.07 \\ 0 & 0 & -12.07 & 28.57 \end{bmatrix},$$

$$C=\begin{bmatrix} 1 & 0 & 0 & 0 & 0 & 0 & 0 & 0 \\ 0 & 1 & 0 & 0 & 0 & 0 & 0 & 0 \\ 0 & 0 & 1 & 0 & 0 & 0 & 0 & 0 \\ 0 & 0 & 0 & 1 & 0 & 0 & 0 & 0 \end{bmatrix} \text{ and } D=0.$$

4.1 Chosen of matrices *Q* and *R*

According to performance requirements for the HFMB, the controller must give favorable suppression to free vibrations, and the energy consumed during control is in secondary consideration. Therefore, *R* can be define as a unit matrix, and then the performance of the controller is adjusted mainly by matrix *Q*. In order to have good damping to the rigid body modes, the damping ratio ξ for each rigid body modes is expected to be between 0.2 and 0.4, which could be obtained by changing the feedback matrix *K*. Since *K* is a function of matrices *R,B* and *P* and *P* is a function of *A,B,Q* and *R,* and that *A* and *B* are known and *R* is unit matrix, *K* is only decided by matrix *Q*.

Fig. 4 and Fig 5 show the variation of the damping ratio ξ with changing of q_i that is the diagonal element of weighing matrix *Q*. From Fig.4, it can be seen that ξ is not sensitive to q_1, q_2, q_3 and q_4 because they are corresponding to the displacements of the rotor. From Fig.5, it can be seen that ξ is sensitive to q_5, q_6, q_7 and q_8 because they are corresponding to the velocities of the rotor. As q_i is in the range of 10^{-5} □ 10^{5}, the damping to the first and third modes reaches to 1, and that for the second and forth modes can also reach to a maximum of 0.25. The maximum value of ξ appears when q_5, q_6, q_7 and q_8 are between $10^{2} \sim 10^{4}$.

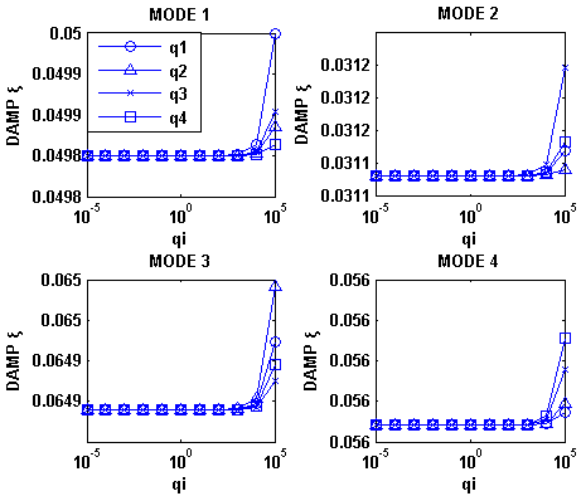

Fig. 4 variation of the damping ratio ξ with q_1, q_2, q_3 and q_4

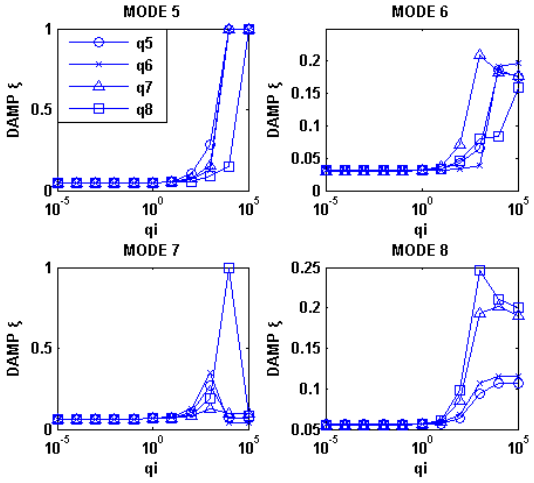

Fig.5 variation of the damping ratio ξ with q_5, q_6, q_7 and q_8

Therefore, choose

$$Q=\begin{bmatrix} I & 0 \\ 0 & q \end{bmatrix}, q=\begin{bmatrix} 400 & 0 & 0 & 0 \\ 0 & 400 & 0 & 0 \\ 0 & 0 & 1000 & 0 \\ 0 & 0 & 0 & 400 \end{bmatrix},$$

and the optimal feedback matrix K would be

$$K=\begin{bmatrix} 782.6 & 318.6 & 3222 & 336.2 & 17.91 & 0.66 & 0.53 & -0.5 \\ -154.1 & 506.8 & 16.3 & 2102 & 0.57 & 17.7 & 1.11 & 1.38 \\ -22367 & 862.8 & -803.1 & 4073 & 1.15 & 1.01 & 25.7 & 2.09 \\ -763.9 & -1558 & -2908 & -545.3 & -0.42 & 0.73 & -1.47 & 17.25 \end{bmatrix}$$

4.2 Design of Kalman filter

Sensor noise v was measured from the eddy current type displacement sensor of an AMB in static suspension. After signal processing, the covariance matrix Rn of the sensor noise can be derived as

$$R_n=\begin{bmatrix} 8.06 & 0 & 0 & 0 \\ 0 & 5.48 & 0 & 0 \\ 0 & 0 & 8.39 & 0 \\ 0 & 0 & 0 & 5.25 \end{bmatrix}\times 10^{-12}$$

The power density of the noise is quit small because of the high SNR of the displacement sensors. Assume that the system noise w is mainly from the gas perturbation and load perturbation, and it is also assumed that the random perturbation force is white and the system noise can be written as

$$F_r=\left[f_{xa}^r, f_{xb}^r, f_{ya}^r, f_{yb}^r \right]^T \tag{13}$$

Then the matrix G and H in Eq.8 would be

$$G=\begin{bmatrix} 0 \\ M_B^{-1} \end{bmatrix}, \quad H=0 \tag{14}$$

The strength of the perturbation force is unknown and is assumed to be at the level of the weight of the rotor. A state white noise produced by software is used in the simulation and each diagonal element of the covariance matrix Q_n is set to 100.

Finally, the gain of Kalman filter can be obtained:

$$L=\begin{bmatrix} 1331.9 & -858.5 & -88.1 & 30.9 & 1434006 & -1236906 & -149908 & 113859 \\ -1263.9 & 1723.0 & 42.7 & -89.6 & -2047990 & 2031637 & 104826 & -179520 \\ -84.7 & 27.9 & 1187.5 & -763.3 & -140791 & 156872 & 1175133 & -961031 \\ 47.5 & -93.6 & -1220.3 & 1626.1 & 187296 & -200825 & -1905172 & 1792689 \end{bmatrix}$$

4.3 Simulation results

The natural frequencies of the rotor-bearing system are in table 3 and the natural modes are shown in fig.6. It can be seen that the rotor is in cylindrical motion in the former four modes and in conical motion in mode4 to mode8. All the eight modes have the required damping.

Table 3 The natural frequencies of the rotor-bearing system

Mode	Eigenvalues	natural frequency (Hz)	Damping ratio
1	-202.4±725.5i	119.88	0.27
2	-284.7±804.6i	135.84	0.33
3	-235.7±1028.8i	167.98	0.22

4	-224.9±1067.7i	173.67	0.21
5	-427.1±1129.78i	192.23	0.35
6	-1404.2±1854.8i	370.25	0.60
7	-483.8±1604.8i	266.77	0.29
8	-1257.3±2106.8i	390.49	0.51

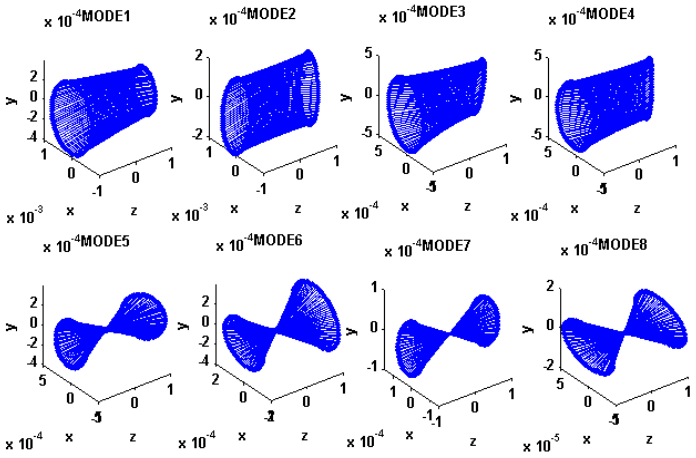

Fig. 6 Natural modes of the rotor

Simulink of Matlab was used for simulation in time domain. The PD control and LQG control are used in the simulation. The PD controller take the diagonal elements of the optimal feedback matrix *K* as PD parameters. A step current of 1A is added into the magnetic bearing, and the responses of displacement *xa* at different power of perturbation forces are shown in Fig.8 and Fig.9. In Fig.8, the power spectrum density(PSD) of the perturbation force is 0.036, and it can be thought as noiseless situation. In this case, the PD control can give nearly the same performance as LQG control. In Fig.9, the PSD of the perturbation force is 360. It can be seen that the LQG control has better performance in noise rejection than the PD control. Moreover, the system with LQG control has quick response and short setting time. Therefore, the HFMB with LQG control could work well at situations with strong perturbation forces.

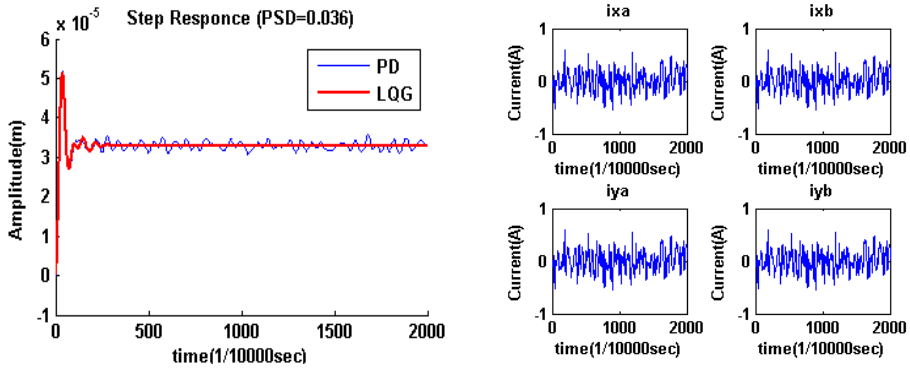

(a) Displacement in *x* direction (b) Control currents of the MB

Fig.8 Step responses of *xa* when the PSD of the perturbation force is 0.036

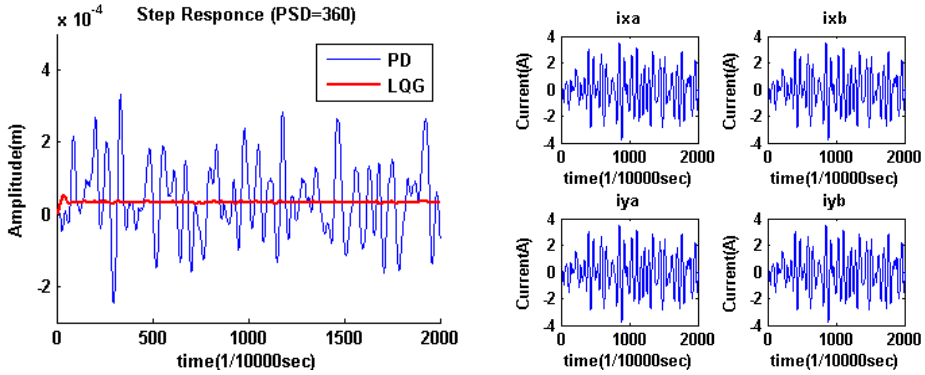

(a) Displacement in *x* direction (b) Currents of the MB

Fig.9 Step responses of *xa* when the PSD of the perturbation force is 360

5. Conclusion

A LQG regulator was designed for the HFMB and simulation was performed to verify the performance of the rotor-bearing system under the LQG control. The simulation results show that the LQG regulator have favorable noise rejection on the HFMB at situations with strong perturbation forces.

References:

[1] Schweitzer G, Traxler A. Mageticlager. Berlin: Springer-Verlag, 1993, 14~16, 48~50, 197~202.

[2] Yunfei Wang. Gas Lubrication Theory and Gas Bearings Design. Beijing, Mechanical Industry Press,1999, 1~143

[3] Ehrich F F, Jacobson S A. Development of high-speed gas bearings for high-power density microdevices. Journal of Engineering for Gas Turbines and Power, 2003, 125(1): 141~148.

[4] Hryniewicz P, Locke D H, Heshmat H. New-generation development rigs for testing high-speed air-lubricated thrust bearings. STLE Tribology Transactions, 2003, 46(4), 556~559.

[5] Liu L X, Teo C J, Epstein A H, et al. Hydrostatic gas journal bearings for micro-turbomachinery. Journal of Vibration and Acoustics, Transactions of the ASME, 2005, 127(2), 157~164.

[6] Yu Lie. Controllable Magnetic Suspension Rotor-bearings system. Beijing: Science Press, 2003, 36~39, 63~80.

[7] Zhiming Zhang, Youpai Xie. The Hydrokinetics Theory of Sliding Bearings. Beijing, China Higher Education Press, 1986, 65~79.

[8] Gang Zhang. Coupled Electromechanical Dynamics of a Rotor-Active Magnetic Bearing System. Xi'an: Xi'an Jiaotong University, 1999, 43~44.

[9] Liu Bao, Wansheng Tang. Modern Control Theory. Beijing, Mechanical Industry Press,2006

[10] Zhenglin Wang, Shengkai Wang. MATLAB/Simulink and Control system simulation. Beijing, Electronic Industry Press, 2008, 293~297.

[11] Geng Haipeng, Study on the Dynamic of an Aerodynamic Compliant Foil Bearing-Rotor System. Xi'an, Xi'an Jiaotong University, 2007, 94.